Electronic Supplementary Information

Thermoelectric stability of Eu- and Na-substituted PbTe

Xinke Wang,[a] Igor Veremchuk,[a] Ulrich Burkhardt,[a] Matej Bobnar,[a] Harald Böttner,[e]

Chang-Yang Kuo,[a,b] Chien-Te Chen,[b] Chun-Fu Chang,[a] Jing-Tai Zhao,[c,d] Yuri Grin[a,*]

[a]Max-Planck-Institut für Chemische Physik fester Stoffe, Dresden 01187, Germany
[b]National Synchrotron Radiation Research Center, 101 Hsin-Ann Road, Hsinchu 30076, Taiwan
[c]School of Materials Science and Engineering, Shanghai University, Shanghai 200444, China
[d]Nanophotonics Center, Texas Tech University, Lubbock, Texas 79409, United States

[e]retired from Fraunhofer-Institut für Physikalische Messtechnik, Freiburg 79110, Germany
[*]corresponding author. E-mail: grin@cpfs.mpg.de.

Table S1. The chemical compositions and lattice parameters of the synthesized $Pb_{0.98-x}Eu_xNa_{0.02}Te$ samples (the real errors of ICP are usually ten times those of the measured errors).

Element	Pb (atom%)	Te (atom%)	Na (atom%)	Eu (atom%)	Composition	Lattice parameter
nominal content	49	50	1		$Pb_{0.98}Na_{0.02}Te$	
before SPS	49.15±0.21	49.82±0.56	1.03±0.01		$Pb_{0.983(4)}Na_{0.021(1)}Te_{0.996(11)}$	6.4577(2)
after SPS	49.26±0.06	49.72±0.07	1.02±0.02		$Pb_{0.985(1)}Na_{0.020(1)}Te_{0.994(1)}$	6.4587(1)
after SPS+LFA	49.16±0.07	49.94±0.16	0.89±0.04		$Pb_{0.983(1)}Na_{0.018(1)}Te_{0.999(3)}$	6.4590(2)
after annealing	50.16±0.09	48.96±0.45	0.88±0.01		$Pb_{1.003(2)}Na_{0.018(1)}Te_{0.979(9)}$	6.4602(2)
nominal content	48.75	50	1	0.25	$Pb_{0.975}Eu_{0.005}Na_{0.02}Te$	
before SPS	48.62±0.15	49.96±0.16	1.15±0.02	0.27±0.002	$Pb_{0.972(3)}Eu_{0.005}Na_{0.023(1)}Te_{0.999(3)}$	6.4589(2)
after SPS	48.55±0.06	50.05±0.16	1.14±0.05	0.27±0.001	$Pb_{0.971(1)}Eu_{0.005}Na_{0.023(1)}Te_{1.001(3)}$	6.4591(2)
after SPS+LFA	48.39±0.16	50.40±0.21	0.94±0.02	0.26±0.002	$Pb_{0.968(3)}Eu_{0.005}Na_{0.019(1)}Te_{1.008(4)}$	6.4595(2)
after annealing	49.66±0.36	49.32±0.42	0.75±0.01	0.28±0.002	$Pb_{0.993(7)}Eu_{0.006}Na_{0.015(1)}Te_{0.986(8)}$	6.4609(2)
nominal content	48.5	50	1	0.5	$Pb_{0.97}Eu_{0.01}Na_{0.02}Te$	
before SPS	48.47±0.18	50.01±0.10	1.07±0.01	0.46±0.005	$Pb_{0.969(4)}Eu_{0.009}Na_{0.021(1)}Te_{1.000(2)}$	6.4596(2)
after SPS	48.43±0.04	50.05±0.39	1.05±0.02	0.47±0.001	$Pb_{0.969(1)}Eu_{0.009}Na_{0.021(1)}Te_{1.001(8)}$	6.4596(1)
after SPS+LFA	48.23±0.01	50.35±0.29	0.95±0.06	0.47±0.001	$Pb_{0.965(1)}Eu_{0.009}Na_{0.019(1)}Te_{1.007(6)}$	6.4604(2)
after annealing	49.30±0.19	49.07±0.20	1.14±0.01	0.50±0.003	$Pb_{0.986(4)}Eu_{0.010(1)}Na_{0.023(1)}Te_{0.981(4)}$	6.4609(2)
nominal content	48.25	50	1	0.75	$Pb_{0.965}Eu_{0.015}Na_{0.02}Te$	
before SPS	48.21±0.12	49.94±0.41	1.10±0.07	0.75±0.02	$Pb_{0.964(2)}Eu_{0.015(1)}Na_{0.022(1)}Te_{0.999\ (8)}$	6.4602(3)
after SPS	48.10±0.26	50.09±0.73	1.08±0.02	0.73±0.002	$Pb_{0.962(5)}Eu_{0.015}Na_{0.022(1)}Te_{1.002(15)}$	6.4595(2)
after SPS+LFA	47.91±0.31	50.60±0.54	0.76±0.01	0.73±0.006	$Pb_{0.958(6)}Eu_{0.015(1)}Na_{0.015(1)}Te_{1.012(11)}$	6.4611(2)
after annealing	48.94±0.14	49.24±0.26	1.06±0.02	0.76±0.001	$Pb_{0.979(3)}Eu_{0.015}Na_{0.021(1)}Te_{0.985(5)}$	6.4618(2)
nominal content	48	50	1	1	$Pb_{0.96}Eu_{0.02}Na_{0.02}Te$	
before SPS	48.01±0.08	49.88±0.32	1.12±0.02	1.00±0.003	$Pb_{0.960(2)}Eu_{0.020}Na_{0.022(1)}Te_{0.998(6)}$	6.4612(2)
after SPS	47.97±0.10	49.94±0.28	1.11±0.11	0.97±0.001	$Pb_{0.959(2)}Eu_{0.019}Na_{0.022(2)}Te_{0.999(5)}$	6.4619(2)
after SPS+LFA	48.01±0.42	50.12±0.42	0.88±0.01	0.99±0.002	$Pb_{0.960(8)}Eu_{0.020}Na_{0.018(1)}Te_{1.002(8)}$	6.4616(2)
after annealing	49.02±0.07	49.20±0.11	0.77±0.04	1.01±0.02	$Pb_{0.980(1)}Eu_{0.020(1)}Na_{0.015(1)}Te_{0.984(2)}$	6.4630(2)
nominal content	47.75	50	1	1.25	$Pb_{0.955}Eu_{0.025}Na_{0.02}Te$	
before SPS	47.52±0.10	49.96±0.16	0.98±0.06	1.34±0.14	$Pb_{0.950(2)}Eu_{0.027(3)}Na_{0.020(1)}Te_{0.999(3)}$	6.4612(3)
after SPS	47.67±0.11	50.05±0.16	1.04±0.02	1.32±0.16	$Pb_{0.953(2)}Eu_{0.026(3)}Na_{0.021(1)}Te_{1.001(3)}$	6.4611(3)
after SPS+LFA	47.67±0.11	50.20±0.24	0.76±0.02	1.37±0.03	$Pb_{0.953(2)}Eu_{0.027(1)}Na_{0.015(1)}Te_{1.004(5)}$	6.4623(2)
after annealing	48.51±0.23	49.24±0.25	0.83±0.04	1.42±0.005	$Pb_{0.970(5)}Eu_{0.028(1)}Na_{0.017(1)}Te_{0.985(5)}$	6.4642(2)

Table S2. Experimental Eu^{3+} and active Na^{+} contents from XAS in units of *x*, as well as experimental active Na^{+} content from Hall measurement in units of *x*. (All data are taken at RT. The error bars of Eu^{3+} (%) reflect the deviations of the fits to the experimental data.)

row	nominal *x*	0	0.005	0.01	0.015	0.02	0.025
1	Experimental Eu^{3+} content from XAS (%)	0	43.2 ± 2.2	31.4 ± 1.6	60.2 ± 3.6	65.1 ± 4.1	39.9 ± 2.2
2	Experimental Eu^{3+} content from XAS (in units of *x*)	0	0.0022(1)	0.0031(1)	0.0090(1)	0.0130(1)	0.0100(1)
3	Experimental active Na^{+} content from XAS (in units of *x*)	0.02	0.0178(1)	0.0169(1)	0.0110(1)	0.0070(1)	0.0100(1)
4	Experimental active Na^{+} content from Hall measurement (in units of *x*)	0.0059(2)	0.0075(3)	0.0070(3)	0.0055(2)	0.0061(2)	0.0055(2)

Row number 1: shows the percentage of Eu^{3+} based on XAS analyses.

Row number 2: shows the Eu^{3+} content in *x* units based on XAS analyses. For sample *x* = 0.01, $Pb_{0.97}^{2+}Eu_{0.0069}^{2+}Eu_{0.0031}^{3+}Na_{0.02}^{+}Te_{1.0}^{2-}$.

Row number 3: shows the active Na^{+} content in *x* units based on XAS analyses.

Row number 4: shows carrier concentration from Hall measurement in the units of *x*.

One may expect that if all Na would be active, the values of row 3 and row 4 would be same. However, this is obviously not the case.

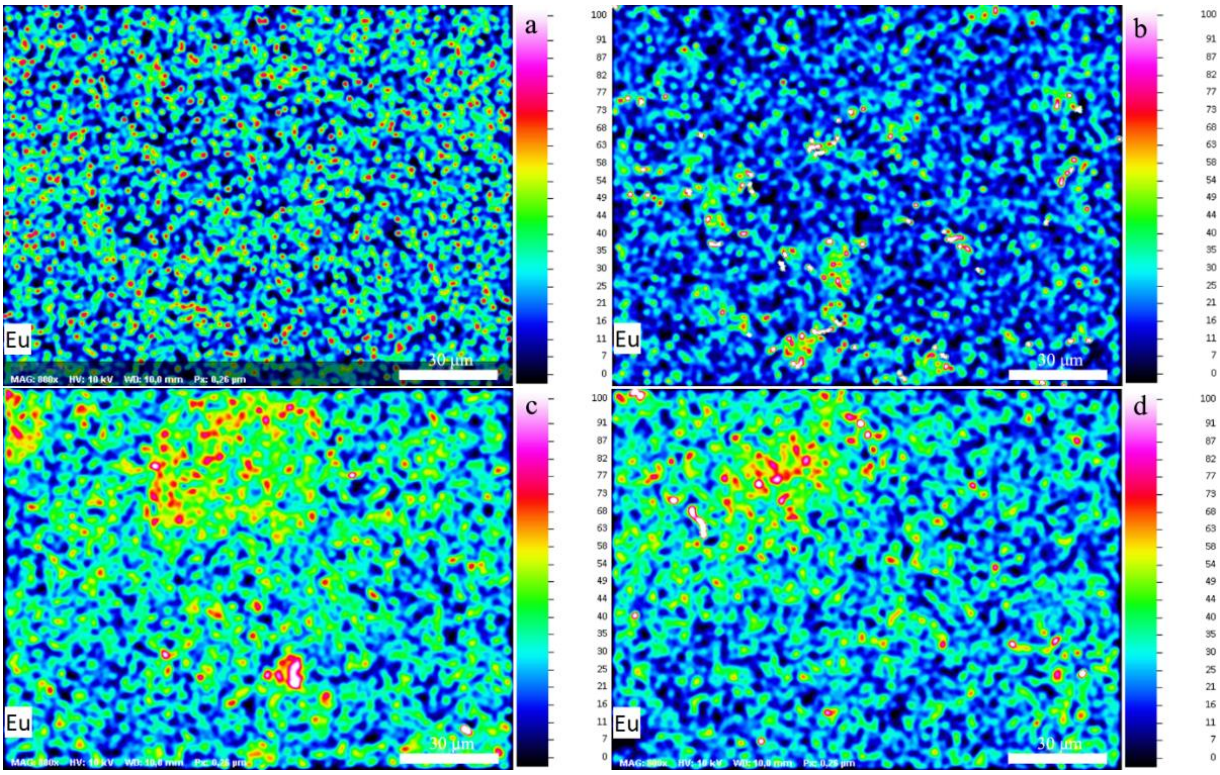

Figure S1. Eu mapping (800× magnification at 10 kV beam voltage) for $Pb_{0.965}Eu_{0.015}Na_{0.02}Te$: (a) before SPS, (b) after SPS, (c) after SPS and LFA, and (d) after annealing at 873 K.

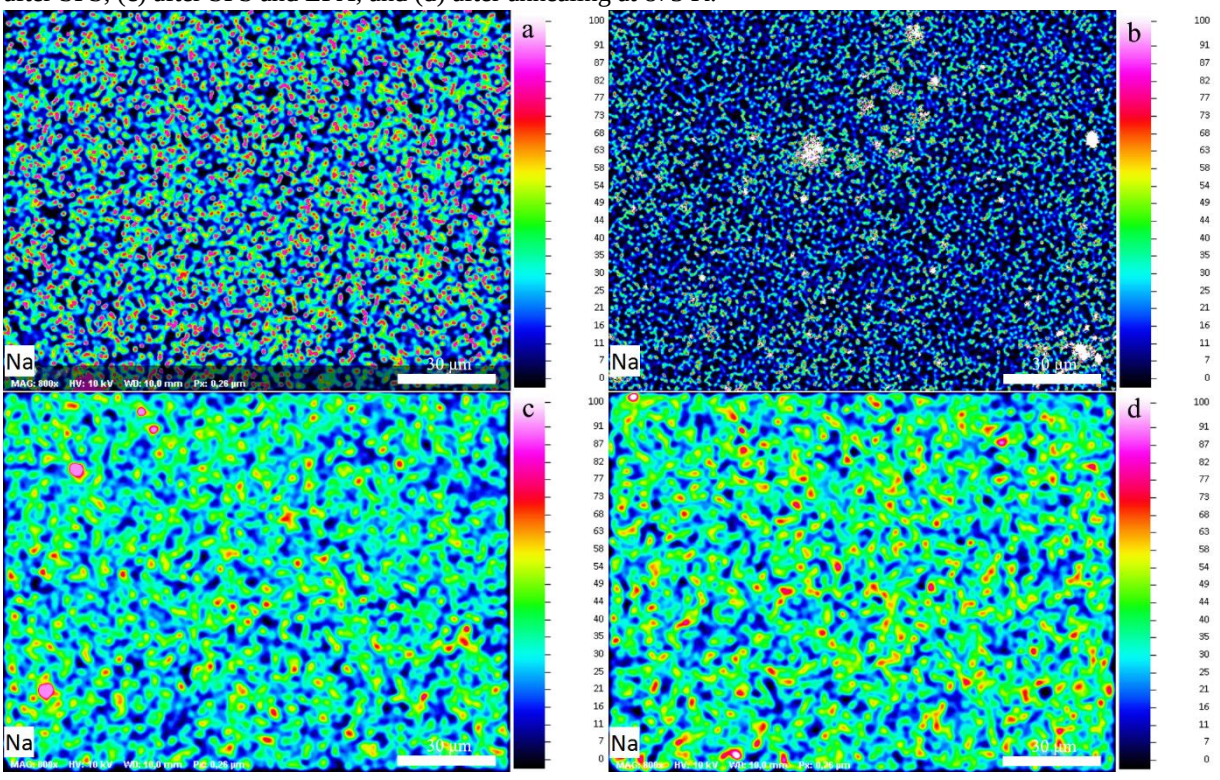

Figure S2. Na mapping (800× magnification at 10 kV beam voltage) for $Pb_{0.965}Eu_{0.015}Na_{0.02}Te$: (a) before SPS, (b) after SPS, (c) after SPS and LFA, and (d) after annealing at 873 K.

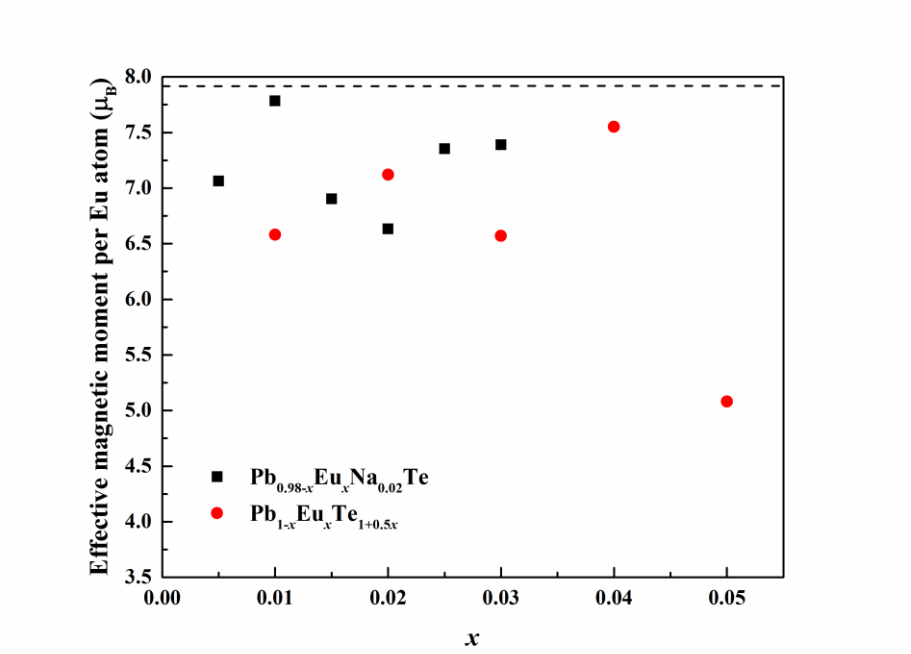

Figure S3. Effective magnetic moment per Eu atom of $Pb_{0.98-x}Eu_xNa_{0.02}Te$ and $Pb_{1-x}Eu_xTe_{1+0.5x}$ before SPS (the dashed line refers to the Eu^{2+} value of 7.9 μ_B).

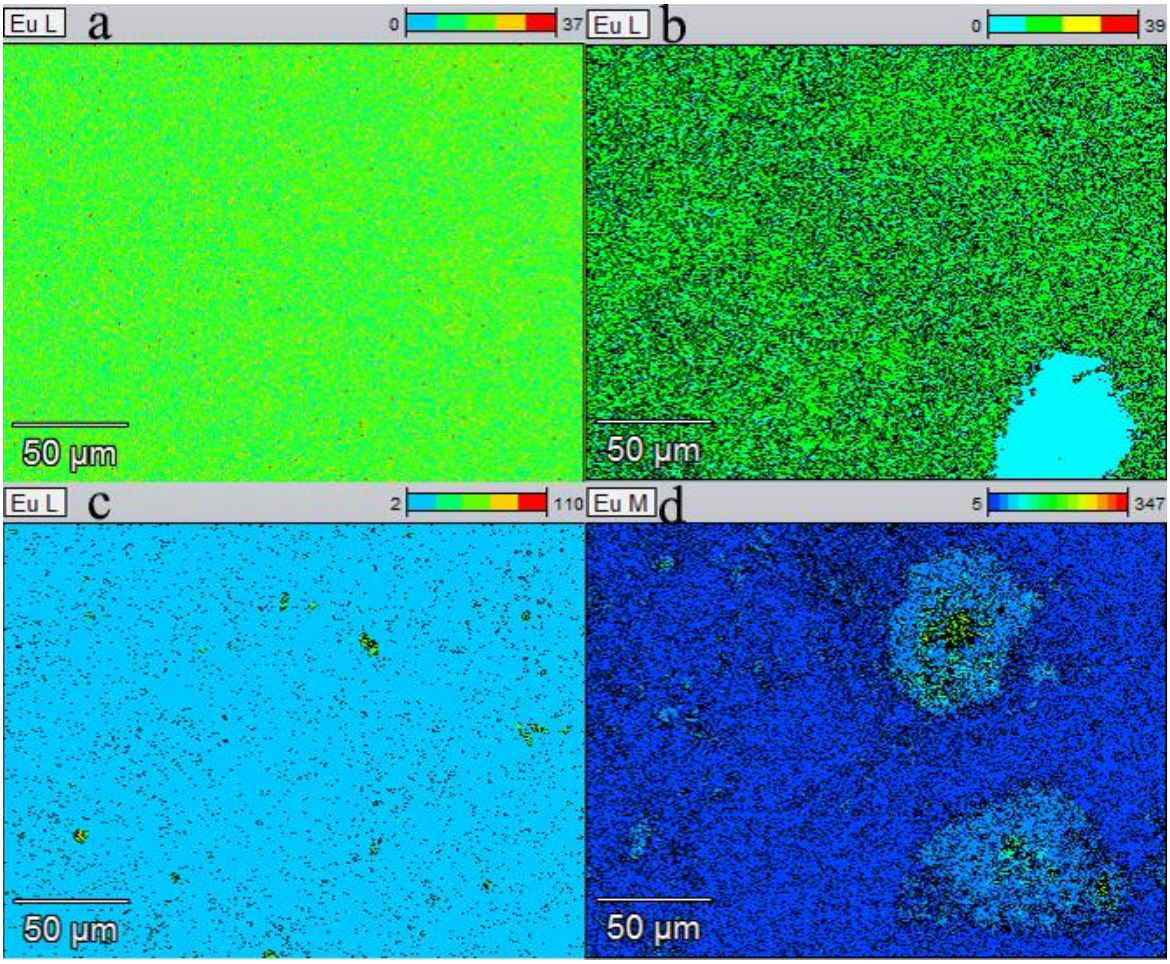

Figure S4. Eu mapping of $Pb_{0.98-x}Eu_xNa_{0.02}Te$ after SPS: (a) x = 0.010, (b) x = 0.015, (c) x = 0.020, and (d) x = 0.025.

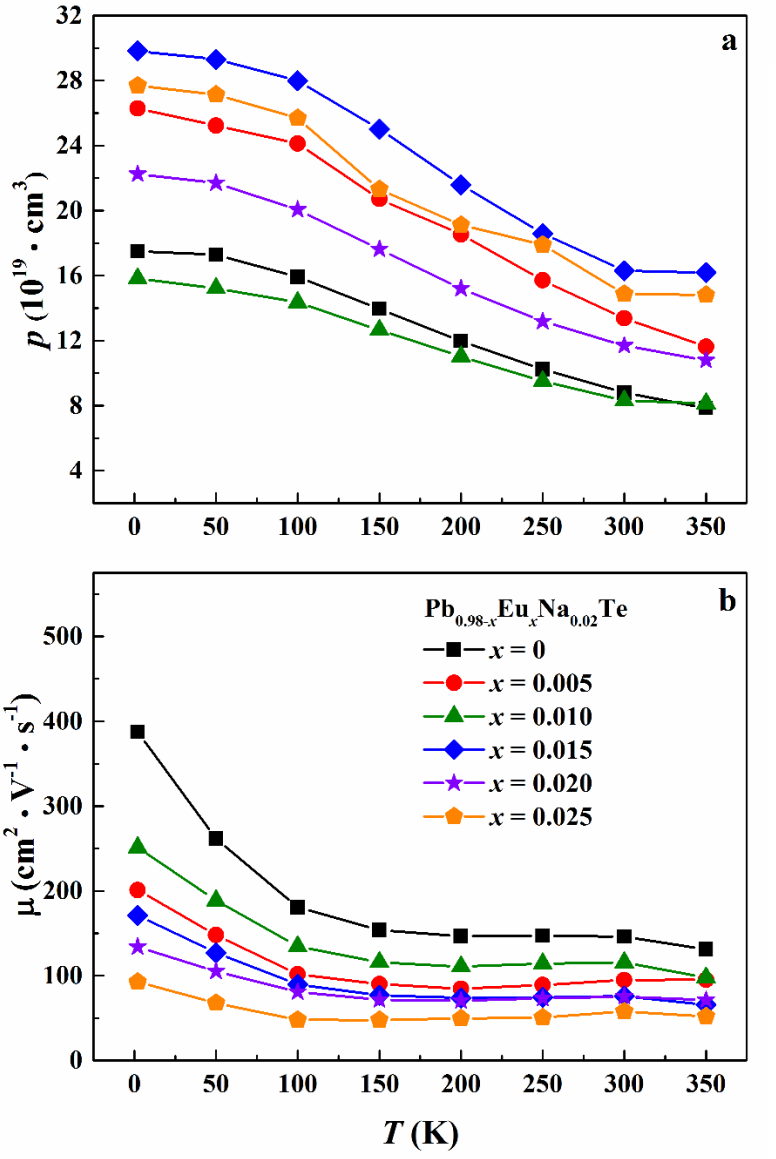

Figure S5. Temperature-dependent (a) Hall carrier concentration p and (b) carrier mobility μ of $Pb_{0.98-x}Eu_xNa_{0.02}Te$ after SPS.

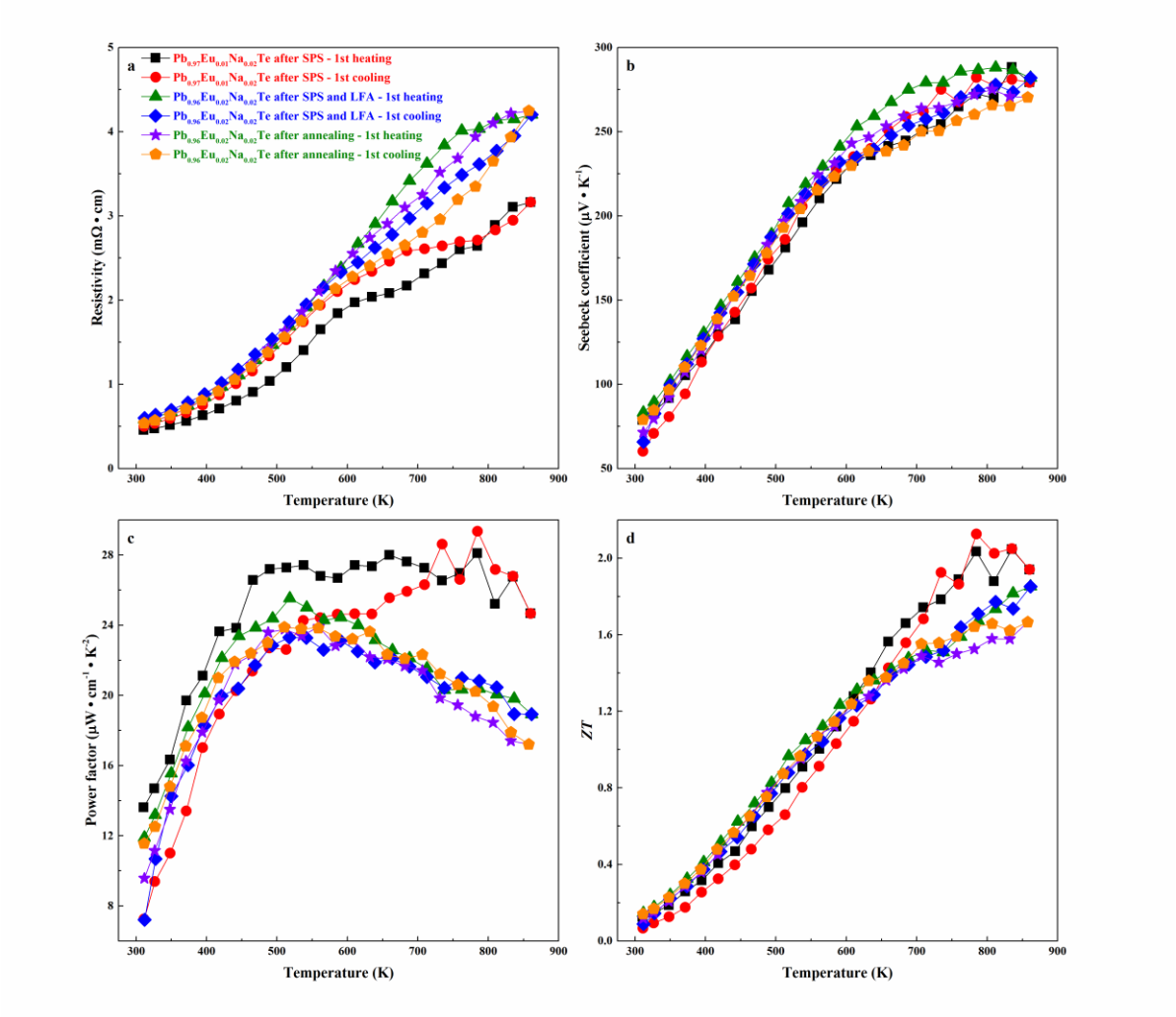

Figure S6. Temperature-dependent (up to 873 K) (a) resistivity, (b) Seebeck coefficient, (c) power factor and (d) thermoelectric figure-of-merit *ZT* for samples: $Pb_{0.97}Eu_{0.01}Na_{0.02}Te$ after SPS, $Pb_{0.96}Eu_{0.02}Na_{0.02}Te$ after LFA, and after annealing.

For the evaluation of these materials in potential high-temperature application, further characterization of the thermal stability at 873 K was carried out. The properties are consistent with our previous measurements (Figure S6), the *ZT* values are also reduced for the samples after additional heat-treatment. The after-SPS specimen becomes bent (Figure S7, right), while the shape does not change for after annealing one (Figure S7, left). However, the surface of all specimens after 873 K ZEM measurements becomes white and removable (Figure S7). The powder XRD pattern of the white surface is presented in Figure S8. It is clear that at high temperature (873 K) and lower pressure (0.1 bar) of Helium atmosphere, the surface of the samples changed. This may be due to evaporation of Te from PbTe for temperatures above 773 K, which is especially likely to occur in vacuum condition.

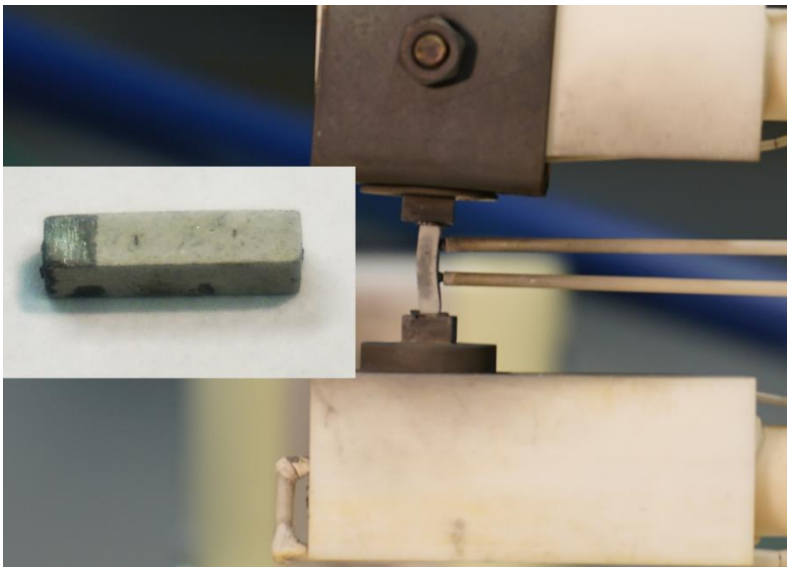

Figure S7. Specimens after ZEM measurement at 873 K: after annealing and ZEM (left), after SPS and ZEM (right).

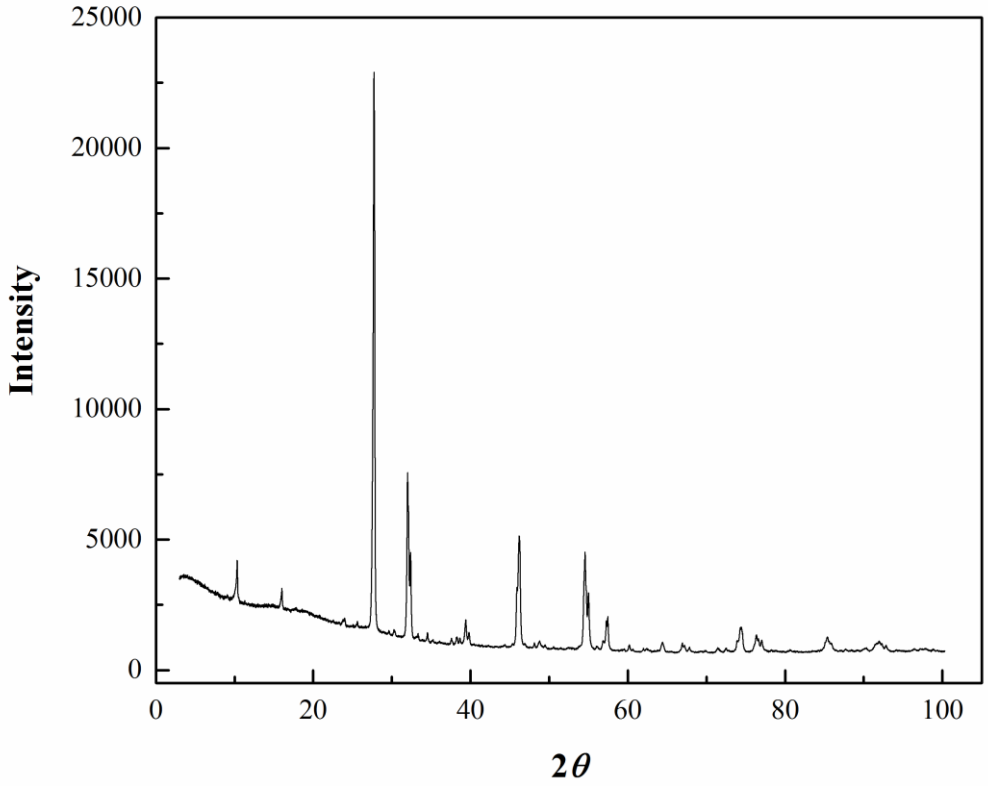

Figure S8. Powder XRD pattern of the white surface from the sample $Pb_{0.96}Eu_{0.02}Na_{0.02}Te$ after 873 K ZEM measurements.